Bandpass filters with conductively coupled eighth-mode SIW resonators

MILOŠ RADOVANOVIĆ[1], SNEŽANA STEFANOVSKI PAJOVIĆ[2], MIODRAG TASIĆ[2], MILKA POTREBIĆ[2,*], DEJAN TOŠIĆ[2]
[1]*School of Electrical Engineering, University of Belgrade, P.O. Box 35-54, 11120 Belgrade, Serbia; Institute of Physics, University of Belgrade, Pregrevica 118, 11080 Belgrade, Serbia*
[2]*School of Electrical Engineering, University of Belgrade, P.O. Box 35-54, 11120 Belgrade, Serbia*

A novel bandpass filter design using eighth-mode substrate integrated waveguide resonators is proposed. Resonators' coupling is realized using a conductive bridge which may be tuned to achieve desired coupling coefficient. This realization overcomes the PCB resolution, i.e. the minimal gap between the resonators. An equivalent circuit is derived for the second-order bandpass filter using a series inductor as the coupling bridge. Design curves of the external quality factor and coupling coefficient are proposed as closed form expressions. Filter prototypes are fabricated on FR4 substrate. The obtained responses show good agreement with 3D electromagnetic simulations, thereby validating the proposed filter design.

(Received December 5, 2021; accepted October 5, 2022)

Keywords: Bandpass filter, Conductively coupled resonators, Eighth-mode SIW resonator, Equivalent circuit, Substrate integrated waveguide

1. Introduction

Substrate Integrated Waveguide (SIW) technology has shown considerable advantages by bridging the gap between printed microwave circuits which are cheap, lightweight, but lossy, and waveguide structures, known as expensive and cumbersome at lower frequencies, but with very low losses. In fact, SIW technology is suitable to implement rectangular waveguides as planar structures [1]. The conditions of equivalence between SIW and dielectric-filled metallic rectangular waveguide are given and explained in [2]. The SIW components exhibit high quality factor, good power handling and may be characterized as electromagnetically shielded structures, similarly as conventional rectangular waveguides. However, due to the side walls structure, leakage losses are possible, resulting in wave attenuation. By proper SIW component design, these losses may be significantly decreased [2]. The details regarding wave propagation and attenuation in SIW have been thoroughly investigated in [3], while the practical aspects and design considerations (substrate selection, fabrication tolerance, power handling) are considered in [4].

Various active and passive components can be implemented using this technology, including resonators and filters which are of interest in our study. The transitions between these components and microstrip lines or coplanar waveguides, may be easily implemented in the same substrate [5]. Different SIW filter solutions have been previously reported in the available open literature. Filters with finite transmission zeros, dual-mode filters, wide band filters, multi-band and reconfigurable filters in SIW technology have been considered in [6]. An overview of the technological advancements and miniaturization trends in SIW filter design is presented in [7]. Dual-mode SIW filter with multiple transmission zeros is presented in [8], while multilayer approach for suppressing higher-order modes of SIW bandpass filter has been introduced in [9].

Although much smaller than traditional waveguide structures, circuits implemented in SIW technology still occupy much greater surface area than other corresponding printed circuits. Thus, there have been made many attempts to reduce their size through various miniaturization techniques [6, 7]. One approach assumes fractional modes, like half-mode (HMSIW), quarter-mode (QMSIW) and eight-mode (EMSIW). Propagation properties of HMSIW have been explained in [10-11]. Various examples of HMSIW filters can be found, like triangular multi-mode HMSIW filter [12], wide band HMSIW filter with defected ground structure (DGS) [13], HMSIW filter loaded with periodic array of longitudinal slots [14] or miniaturized fan-shaped HMSIW filter with wide stopband [15]. Different coupling mechanisms and feeding techniques for QMSIW filters have been presented in [16]. Filter consisting of cascaded, inductively coupled, QMSIW cavities has been demonstrated in [17], while filter using fractal-shape quarter substrate integrated waveguide (QSIW) resonators can be found in [18]. Compact modified single-band and dual-band QMSIW filters have been considered in [19]. Filter obtained by coupling EMSIW resonators has been introduced in [20], filter using single EMSIW cavity in [21], multi-layered EMSIW filter in [22] and compact single-layer EMSIW filter with improved out-of-band rejection in [23]. The compactness of the SIW filters may be achieved by adding various planar structures, like SIW loaded with SIR-CSRR (Stepped-Impedance Resonator - Complementary Split Ring Resonators) unit cells [24] or with CMRC (Compact Microstrip Resonant Cell) [25]. An overview of different techniques for SIW

cavities miniaturization, as well as the use of innovative materials for the SIW filter design, with the emphasis on the emerging IoT (Internet of Things) applications, is demonstrated and exemplified in [26].

When used in filters, SIW resonators are usually mutually coupled and interfaced with external lines or other resonators, implemented in various planar technologies, like microstrip, stripline and coplanar waveguides, by means of capacitive, inductive or conductive coupling. Traditional SIW coupling between resonators is mainly achieved as inductive, with a gap in electric wall, by removing several vias, or with a pair of S-shaped slots encompassing two vias [27]. With HMSIW, QMSIW and EMSIW, coupling between resonators has been either capacitive [20] or inductive [17]. Hybrid structures, based on combining SIW and microstrip [28] or stripline [29] technologies, use capacitive, inductive or mixed coupling too. The usage of conductive coupling for filter design in planar technologies has been exemplified in [30-32]. Furthermore, the advantages of conductive coupling, compared to capacitive and inductive coupling, have been shown in an example of two split-ring resonators in [33].

In this paper we demonstrate filter design using conductive coupling between EMSIW resonators, as an alternative which can achieve broader range of coupling coefficients and have less strict requirements on technology resolution. Unlike capacitive or inductive coupling, conductive coupling overcomes the limitation regarding a feasible gap width (which depends on the printing resolution) between the coupled components. Proposed conductive coupling solution exhibits design flexibility in terms of possibility to tune the coupling coefficient. Basic mode of propagation TE_{10} is considered. Besides the three-dimensional electromagnetic (3D EM) model, the equivalent microwave circuit is generated as well. Two prototype filters, with different positions of the coupling bridge between the resonators, are fabricated to experimentally verify the proposed approach. The obtained simulated and measured results show good mutual agreement, thus confirming a novel SIW filter solution.

2. Eighth-mode SIW resonators

An important advantage of SIW circuits is a fact that their behaviour can be easily approximated by that of rectangular waveguides, which have been studied for many decades, and whose field has a simple closed form solution.

The SIW geometry is defined by three parameters: the via diameter d, the distance between the centres of the two corresponding vias within the opposite walls w (width of the waveguide), and the distance between the centres of two corresponding vias within the same wall s (longitudinal spacing). As the SIW structure emulates the rectangular waveguide, its width w is related to the cutoff frequency of the fundamental SIW mode and consequently to the operation frequency band. The via diameter d is usually less than $w/8$ and is recommended to avoid possible band-gap effects. The longitudinal spacing s affects the confinement of the electromagnetic field, because it determines the gap-width (s - d) between pairs of vias. The minimum value of s is d, which means that there is no gap and the metallic wall is perfect. If the value of s increases, the gaps become larger and the field confinement degrades. Usually, s is less than 2.5 d, and the typical choice is when s is equal 2 d [1].

This approximation was described by introducing the equivalent width of the SIW [3] thereby substituting the wall of vias with a perfect electric conductor (PEC) plane. The following equation was proposed for the equivalent width, w_{eff}, calculation:

$$w_{\text{eff}} = w - 1.08\frac{d^2}{s} + 0.1\frac{d^2}{w}. \tag{1}$$

Same formula can be used for determining the equivalent length, L_{eff}, in rectangular SIW resonators. Their resonances can be predicted using formula for the classic rectangular (square) resonator:

$$f_{\text{res}} = \frac{c_0}{w_{\text{eff}}\sqrt{2\varepsilon_{\text{r}}}}. \tag{2}$$

Cutting a SIW resonator (SIWR) with a perfect magnetic conductor (PMC) sheet, perpendicular to the magnetic field lines, would not change the field structure and the resonant frequency. This can be done along one or both symmetry planes of rectangular SIWR, resulting in HMSIW resonator (HMSIWR) and QMSIW resonator (QMSIWR), respectively, or even along all four symmetry planes for square SIWR, resulting in EMSIW resonator (EMSIWR) (Fig. 1).

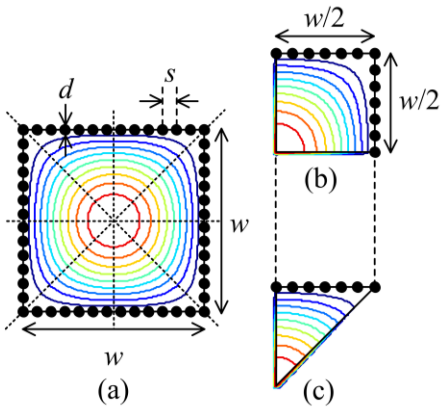

Fig. 1. Square (a) and fractional (b, c) configurations of SIW resonator with its electric field symmetries which could be replaced by magnetic walls. Black filled circles represent via holes. Drawing (b) shows QMSIWR, and (c) shows EMSIWR

Additional correction to the equivalent width, due to the edge effects introduced by cutting half mode symmetry plane, can be made in accordance with [11], but that is not of interest for further consideration here.

The unloaded Q-factor of the EMSIWR is computed as follows:

$$Q_0 = Q_{\text{L}} / \left(1 - \left|S_{21}(\text{j}\omega_0)\right|\right), \tag{3}$$

where the loaded Q-factor of the resonator is inversely proportional to the 3-dB bandwidth i.e.

$$Q_{\mathrm{L}} = \omega_0/(\omega_2 - \omega_1). \tag{4}$$

$S_{21}(\mathrm{j}\omega_0)$ is the value of the S_{21} parameter at the considered resonant frequency ω_0 which denotes the angular frequency in rad/s.

The equivalent-circuit model of the EMSIWR is shown in Fig. 2. The values of the circuit elements are calculated using following equations as proposed in [34, 35]:

$$R = Z_0 |S_{21}(\mathrm{j}\omega_0)|/(2(1-|S_{21}(\mathrm{j}\omega_0)|)), \tag{5}$$

$$L = B_0 Z_0 |S_{21}(\mathrm{j}\omega_0)|/(2\omega_0^2), \tag{6}$$

$$C = 2/(B_0 Z_0 |S_{21}(\mathrm{j}\omega_0)|), \tag{7}$$

where B_0 is the bandwidth in rad/s, which corresponds to the unloaded Q-factor as $B_0 = \omega_0/Q_0$. The impedances of ports (Z_0) correspond to the value of 50 Ω.

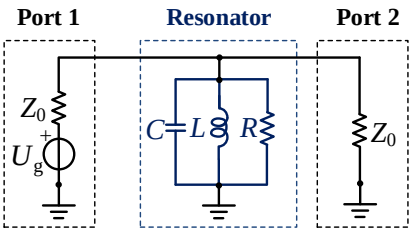

Fig. 2. Equivalent-circuit model of EMSIWR

3. Bandpass filter design with conductively coupled eighth-mode SIW resonators

Herein we propose a bandpass filter with conductive coupling between the resonators using SIW technology, as shown in Fig. 3. In this case, it should be distinguished two types of coupling between resonators. First one is a coupling through a gap between resonators, i.e. through fringe fields which are magnetic or electric or even the combination of both. Consequently this type of coupling is named magnetic, electrical or mixed. Second one is a conductive coupling based on a conductive bridge which connects two resonators mechanically and electrically.

The main idea is to separate these two coupling types i.e. to neglect coupling through the gap between resonators when using a conductive ones. We have chosen the gap between resonators to be enough wide that the coupling through the gap could be neglected. In that case, only the bridge position is responsible for the intensity of the coupling.

Two EMSIW resonators are coupled using a conductive bridge of length s_b and width w_b. The bridge length s_b is equal to the gap width between two resonators. This realization is simple for tuning a precise coupling between resonators. One can solely find the optimal bridge position to achieve the desired coupling. In case the bridge is not used to span the gap between the resonators, the maximum coupling is determined by the printing resolution of planar microwave structures, i.e. it is limited by the feasible gap width. In fact, the main contribution of the use of conducting coupling is that the printing resolution does not impose the coupling boundary anymore.

In order to present advantages of using conductive coupling, we designed two second-order bandpass filters (denoted as Filter 1 and Filter 2). Filters have centre frequencies at 1.29 GHz and 1.39 GHz, and relative bandwidths of 13 % and 29 %, respectively.

In this study, we use the FR-4 substrate with the following parameters: $\varepsilon_r = 4.2$, $\tan\delta = 0.02$, thickness $h = 1.575$ mm and metallization thickness $t = 0.017$ mm. The metal losses, due to the skin effect and surface roughness, are taken into account by setting the conductivity $\sigma = 20$ MS/m.

Dimensions of the presented filters are given in Table 1.

Table 1. Filter dimensions (in mm)

Parameter	Filter 1	Filter 2
$w/2$	42.849	
w_0	3.3	
s	1.5	
d	1.0	
s_b	1.2	
w_b	1.1 w_0	
P	45.0	
D	60.0	
p_0	20.84	12.44
p_0/P	0.463	0.276
p_b	29.70	20.15
p_b/D	0.495	0.336

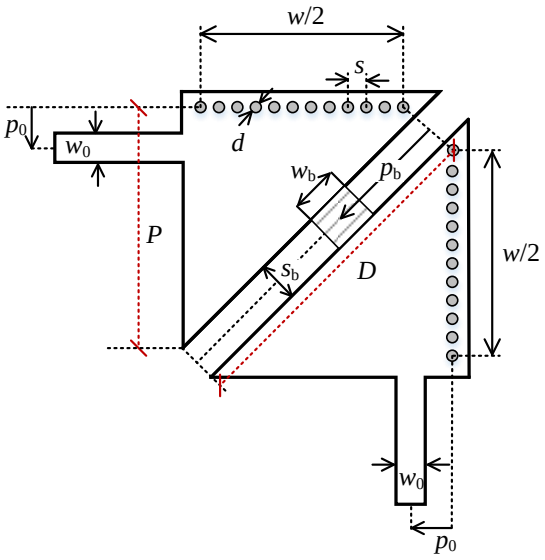

Fig. 3. Bandpass filter with conductively coupled eighth-mode SIW resonators

Full 3D electromagnetic analysis is performed using the electric field surface integral equations discretized by the method of moments [36]. The 3D EM model of the bandpass filter is shown in Fig. 4.

The corresponding circuit parameters of ESIWR (for both filters) are: $R = 2.2426\ \Omega$, $L = 6.6680$ pH, $C = 2.4947$ nF, $Q_0 = 43.3773$. These values are obtained using equations (3)-(7).

The equivalent circuit of the filters using EMSIW resonators is shown in Fig. 5. The loaded resonators are modelled with ideal transformers. The bridge coupling between resonators is modelled with two transformers and a series inductor with inductance L_b (about 1.5 nH). Parameters of the ideal transformers are $N \approx Q_e$ and $M \approx k$, where Q_e is the external quality factor and k is the coupling coefficient. From even- and odd-mode equivalent network analysis, it can be found that the even-mode frequency is equal to the resonator frequency:

$$f_{res} = f_{even} = \frac{f_0^2}{f_{odd}} = f_0\left(\frac{1-k}{1+k}\right)^{0.25}, \qquad (8)$$

where the coupling coefficient k is defined with

$$k = \left(f_{odd}^2 - f_{even}^2\right)\Big/\left(f_{odd}^2 + f_{even}^2\right). \qquad (9)$$

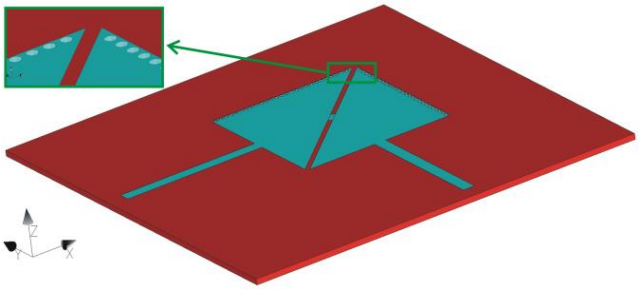

Fig. 4. 3D EM model of the bandpass filter with conductively coupled eighth-mode SIW resonators (color online)

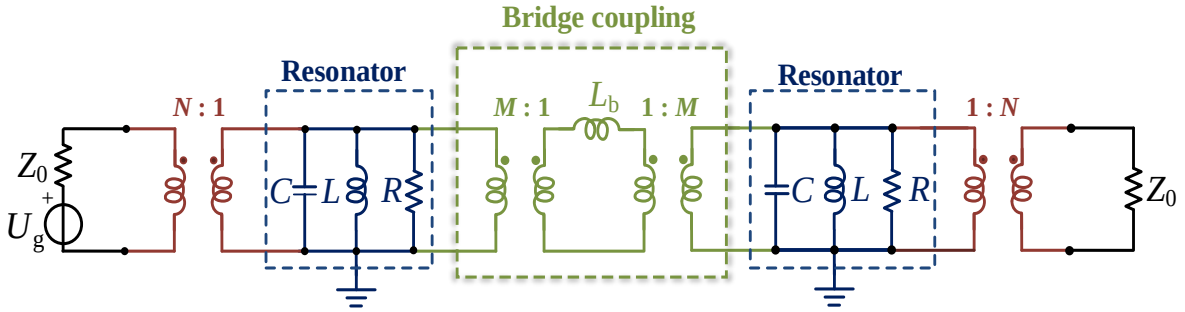

Fig. 5. Equivalent circuit of the bandpass filter with conductively coupled eighth-mode SIW resonators (color online)

In fact, the main difference of using conductive coupling to inductive or capacitive one is that the centre frequency of the filter (f_0) will be different from the resonator frequency (f_{res}).

The use of conductive coupling has the following influence on the filter responses: the lower band-edge frequency will remain fairly constant and independent of the coupling coefficient k, while the upper frequency will change with it. Such behaviour is confirmed by the filter responses (Fig. 6) obtained by performing full-wave simulations on the 3D EM models and circuit-level simulations based on the equivalent circuit, for numerical values given in Table 2.

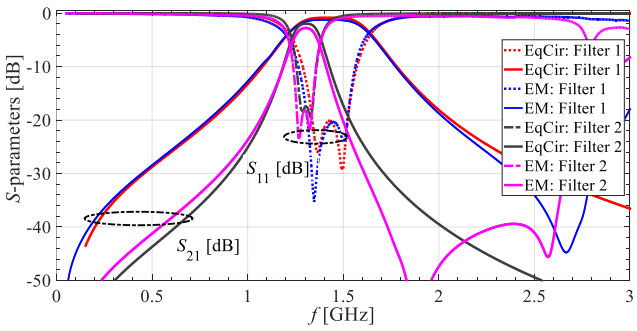

Fig. 6. Comparison of frequency responses for Filter 1 and Filter 2 (EqCir - equivalent circuit; EM - 3D EM model) (color online)

Design curve of external quality factor for the eighth-mode SIW resonator is shown in Fig. 7. The quality factor is presented as a function of normalized position of the feed line $z = p_0/P$. The parameter P is shown in Fig. 3. The following curve fits well to the set of calculated and experimental values:

$$Q(z) = q_0 \sin^{-2}(\frac{\pi}{2} z), \tag{10}$$

for the lower values of z, where $q_0 = 0.65$. For the entire range, $0 < z < 1$, the design curve might be presented with expression

$$Q(z) = q_1 z^{q2} + q3, \tag{11}$$

where the coefficients are $q_1 = 0.7059$, $q_2 = -2.124$ and $q_1 = 3.209$.

Table 2. Two filters with base resonator frequency of 1.21 GHz

Parameter	Filter 1	Filter 2
center frequency f_0	1.39 GHz	1.29 GHz
reflection @ f_0	-20.8 dB	-21 dB
transmission @ f_0	-1.1 dB	-2.3 dB
relative bandwidth	29 %	13 %
bridge position	0.495	0.336
port position	0.463	0.276

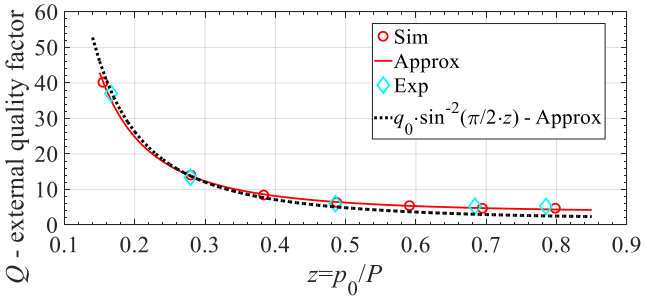

Fig. 7. Design curve of the external quality factor for the eighth-mode SIW resonator (as functions of normalized port position)(color online)

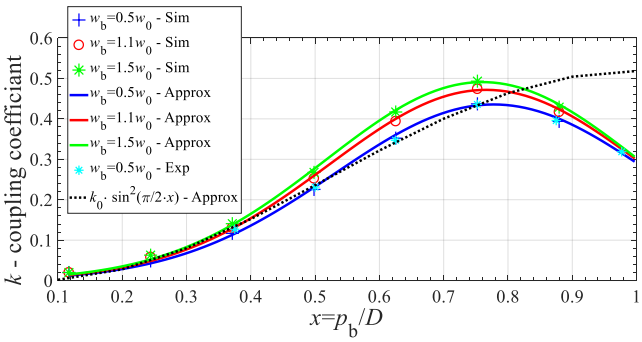

Fig. 8. Design curve of coupling coefficient k for the conductively coupled eighth-mode SIW resonators (as functions of normalized bridge positions) (color online)

Design curves of the coupling coefficient for the two eighth-mode SIW resonators are shown in Fig. 8. The coupling coefficient depends only on the bridge position between resonators, notated as a dimension p_b. The initial position of the bridge (p_b=0) is placed in between the two rows of metalized cylindrical holes which connects the two ground planes and emulate the metallic side walls of standard waveguides. The coupling coefficients are presented as functions of normalized bridge position $x = p_b/D$, where the parameter D is hypotenuse length of right triangular resonator as shown in Fig. 3. Three curves are calculated for a different bridge width w_b. We have used w_b equal to $0.5w_0$, $1.1w_0$ and $1.5w_0$. The calculated and experimental coupling values are represented by dot charts (see Fig. 8). The position of the maximum coupling coefficient is constant and it is not function of the metallic bridge width w_b, while maximal value increases with increasing of width w_b. The maximum position is placed around the normalized bridge position 0.75 ($x = p_b/D$). Fitting to each set of the experimental values might be represented by the curve

$$k(x, y) = A(y) \cdot \mathrm{e}^{-\left(\frac{x - B(y)}{C(y)}\right)^2}. \tag{12}$$

The variable y is a normalized bridge width, $y = w_b/D$. Parameters $A(y)$, $B(y)$ and $C(y)$ are functions of the normalized bridge width (y) and might be fitted with the following polynomials:

$$A(y) = a_1 y^2 + a_2 y + a_3 \tag{13}$$

with the coefficients $a_1 = -3.969$, $a_2 = 1.438$, $a_3 = 0.3988$,

$$B(y) = b_1 y^2 + b_2 y + b_3 \tag{14}$$

with the coefficients $b_1 = 1.631$, $b_2 = -0.4967$, $b_3 = 0.7901$, and

$$C(y) = c_1 y^2 + c_2 y + c_3 \tag{15}$$

with the coefficients $c_1 = 1.359$, $c_2 = -0.2408$, $c_3 = 0.3557$.

For the lower values of x and $w_b = 0.5w_0$, the coupling coefficient can be presented as

$$k(x) = k_0 \sin^2(\frac{\pi}{2} x), \tag{16}$$

where $k_0 = 0.8$.

The use of ideal transformers, for which transformation ratio is proportional to electric field strength, at the point of placement of filter bridge and ports, results in $\sin^{-2}$ and $\sin^2$ type functions approximating the external Q-factor and resonator coupling coefficient k, versus the port position and normalized bridge, respectively. These approximations are shown in Figs. 7 and 8. However, deviation from this can occur for lower values of the Q-factor because of losses, and higher values of the coupling coefficient k due to virtual coupling of the bridge to its image in PMC symmetry planes.

4. Bandpass filter prototype and experimental verification

Two second-order bandpass filters using conductively coupled EMSIW resonators, with differently positioned feeding ports and coupling bridges, are fabricated on FR4 substrate (Fig. 9), to experimentally verify the proposed design. The obtained measured responses are compared to the simulated ones (Fig. 10), showing good agreement, particularly in the pass bands, and validating the presented solution for SIW filters design.

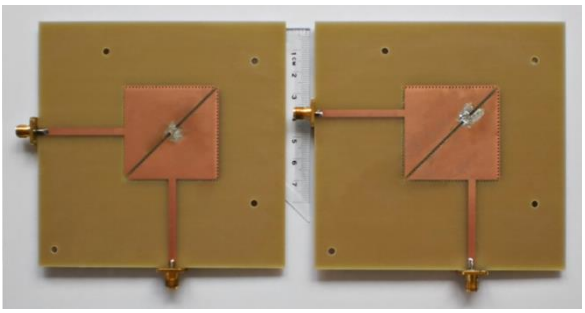

Fig. 9. Photograph of the two filters fabricated on FR4 substrate Filter 1(left) and Filter 2 (right)

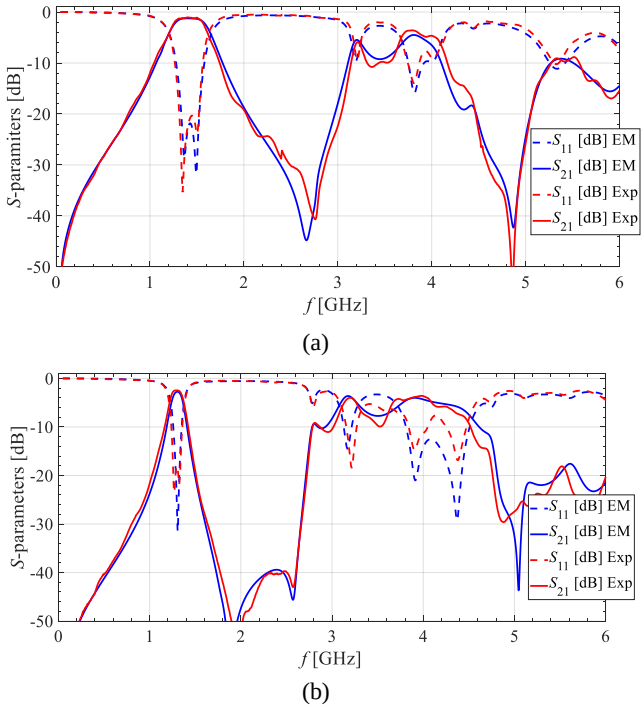

Fig. 10. Comparison of the simulated and measured results for: (a) Filter 1, (b) Filter 2 (color online)

5. Conclusion

A novel bandpass filter design using two conductively coupled EMSIW resonators has been presented. Conductive coupling has been performed using bridge across the gap between the resonators. Such design has overcome the limitation imposed by the printing resolution of planar microwave structures, thereby confirming the advantage of the use of conductive coupling over capacitive and inductive one, for the SIW filter design.

A simple equivalent circuit has been derived for the considered filter. An inductor and ideal transformers with adequately chosen parameters, i.e. transformation ratios, have successfully modelled the bridge coupling, thus providing the possibility to tune the coupling by solely varying the bridge position.

Design curves of the external quality factor and the coupling coefficient represent another contribution of this research. Analytical expressions have been proposed for the external quality factor, as a function of normalized port position, and for the coupling coefficient, as a function of normalized bridge position. These expressions apply to the entire range of normalized port and bridge positions, for the considered filter.

The proposed filters, with different port and bridge positions, have been fabricated and their responses have been experimentally verified, showing good agreement with the results obtained by 3D EM simulations. In this manner, the presented solution has been validated for the SIW filter design using conductive coupling.

Considered filters were designed for the centre frequencies between 1 GHz and 2 GHz. However, frequency range is not a limiting factor to reuse the same concept presented here for other SIW components. Future research might focus on the application of such design for the filters operating in different frequency bands, thereby scaling their size accordingly, so they could be used in the systems developed for the emerging technologies. Also, the authors consider design improvement in terms of undesired higher-bands suppression.

Acknowledgments

This work was supported in part by the Ministry of Education, Science and Technological Development of the Republic of Serbia, project no. 2022/200103, and by the Innovation Fund from the budget of the Republic of Serbia from the division of the Ministry of Education, Science and Technological Development, through the Serbia Competitiveness and Jobs Project (loan agreement with the World Bank).

References

[1] R. Garg, I. Bahl, M. Bozzi, “Microstrip Lines and Slotlines”, 3rd ed., Artech House, Boston, MA (2013).
[2] X.-P. Chen, K. Wu, IEEE Microw. Mag. **15**(5), 108 (2014).
[3] F. Xu, K. Wu, IEEE T. Microw. Theory **53**(1), 66 (2005).
[4] X.-P. Chen, K. Wu, IEEE Microw. Mag. **15**(7), 75 (2014).
[5] D. Deslandes, K. Wu, IEEE T. Microw. Theory **51**(2),

593 (2003).
[6] X.-P. Chen, K. Wu, IEEE Microw. Mag. **15**(6), 121 (2014).
[7] A. Iqbal, J. J. Tiang, S. K. Wong, M. Alibakhshikenari, F. Falcone, E. Limiti, IEEE Access **8**, 223287 (2020).
[8] P. Chu, W. Hong, M. Tuo, K.-L. Zheng, W.-W. Yang, F. Xu, K. Wu, IEEE T. Microw. Theory **65**(3), 824 (2017).
[9] D. Jia, Q. Feng, Q. Xiang, K. Wu, IEEE Microw. Wirel. Compon. Lett. **26**(9), 678 (2016).
[10] W. Hong, B. Liu, Y. Wang, Q. Lai, H. Tang, X. X. Yin, Y. D. Dong, Y. Zhang, K. Wu, Proc. Joint 31st Intern. Conf. on Infrared Millimeter Waves and 14th Intern. Conf. on Teraherz Electronics, Shanghai, China, p. 219 (2006).
[11] Q. Lai, C. Fumeaux, W. Hong, R. Vahldieck, IEEE T. Microw. Theory **57**(8), 1996 (2009).
[12] M. Li, C. Chen, X. Zhang, W. Chen, Proc. The 37th Progress in Electromagnetic Research Symposium, Shanghai, China, p. 3809 (2016).
[13] Z. Yang, Z. Wang, J. Dong, Y. Liu, T. Yang, Proc. 2015 IEEE Intern. Conf. on Signal Processing, Communications and Computing, Ningbo, China, p. 1 (2015).
[14] S. Moitra, P. S. Bhowmik, AEU-Int. J. Electron. C. **70**(12), 1593 (2016).
[15] H.-Y. Xie, B. Wu, L. Xia, J.-Z. Chen, T. Su, IEEE Microw. Wirel. Compon. Lett. **30**(8), 749 (2020).
[16] S. Moscato, C. Tomassoni, M. Bozzi, L. Perregrini, IEEE T. Microw. Theory **64**(8), 2538 (2016).
[17] Z. Zhang, N. Yang, K. Wu, Proc. IEEE Radio and Wireless Symposium, San Diego, CA, USA, 95 (2009).
[18] S. Zhang, T. J. Bian, Y. Zhai, W. Liu, G. Yang, F. L. Liu, Microwave J. **55**(5), 200 (2012).
[19] Y.-Z. Zhu, W.-X. Xie, X. Deng, Y.-F. Zhang, ACES J. **32**(2), 163 (2017).
[20] G. Yang, W. Liu, F. Liu, Proc. Intern. Conf. on Microwave and Millimeter Wave Technology (ICMMT), Shenzhen, China, p. 1 (2012).
[21] Y. Zhu, Proc. XXXIth URSI General Assembly and Scientific Symposium (URSI GASS), Beijing, China, p 1 (2014).
[22] Y. Zhu, Proc. IEEE 6th Intern. Symposium on Microwave, Antenna, Propagation, and EMC Technologies (MAPE), Shanghai, China, 620 (2015).
[23] L. Li, Z. Wu, K. Yang, X. Lai, Z. Lei, IEEE Microw. Wirel. Compon. Lett. **28**(5), 407 (2018).
[24] M. Danaeian, K. Afrooz, A. Hakimi, AEU-Int. J. Electron. C. **84**, 62 (2018).
[25] L. Huang, W. Wu, X. Zhang, H. Lu, Y. Zhou, N. Yuan, AEU-Int. J. Electron. C. **82**, 420 (2017).
[26] C. Tomassoni, M. Bozzi, Radioengineering **26**(3), 633 (2017).
[27] X.-P. Chen, K. Wu, IEEE T. Microw. Theory **56**(1), 142 (2008).
[28] Y. Zhu, Y. Dong, IEEE Microw. Wirel. Compon. Lett. **31**(7), 841 (2021).
[29] Y. Zhu, Y. Dong, IEEE Microw. Wirel. Compon. Lett. **30**(5), 465 (2020).
[30] Y.-H. Cho, G. M. Rebeiz, IEEE T. Microw. Theory **62**(11), 2626 (2014).
[31] C. J. Kikkert, Proc. IEEE Region 10 TENCON 2005, Melbourne, Qld., Australia, paper 1568965073, p. 1 (2005).
[32] E. J. Naglich, J. Lee, D. Peroulis, W. J. Chappell, IEEE T. Microw. Theory **58**(12), 3770 (2010).
[33] I. Al-Naib, E. Hebestreit, C. Rockstuhl, F. Lederer, D. Christodoulides, T. Ozaki, R. Morandotti, Phys. Rev. Lett. **112**(18), 183903 (2014).
[34] S. Stefanovski, M. Potrebić, D. Tošić, Proc. 11th Intern. Conf. on Telecommunication in Modern Satellite, Cable and Broadcasting Services (TELSIKS), Niš, Serbia, p. 257 (2013).
[35] A. Khanna, Y. Garault, IEEE T. Microw. Theory, **31**(3), 261 (1983).
[36] WIPL-D Pro 17.0, 3D Electromagnetic Solver, WIPL-D d.o.o., Belgrade, Serbia, http://www.wipl-d.com (2020).

*Corresponding author: milka_potrebic@etf.rs